LKB1 induces apical trafficking of Silnoon, a monocarboxylate transporter, in *Drosophila melanogaster*

Cholsoon Jang,[1,2] Gina Lee,[1,2] and Jongkyeong Chung[1,2]

[1]National Creative Research Initiatives Center for Cell Growth Regulation and [2]Department of Biological Sciences, Korea Advanced Institute of Science and Technology, Yusong-gu, Taejon 305-701, Korea

Silnoon (Sln) is a monocarboxylate transporter (MCT) that mediates active transport of metabolic monocarboxylates such as butyrate and lactate. Here, we identify Sln as a novel LKB1-interacting protein using *Drosophila melanogaster* genetic modifier screening. Sln expression does not affect cell cycle progression or cell size but specifically enhances LKB1-dependent apoptosis and tissue size reduction. Conversely, down-regulation of Sln suppresses LKB1-dependent apoptosis, implicating Sln as a downstream mediator of LKB1. The kinase activity of LKB1 induces apical trafficking of Sln in polarized cells, and LKB1-dependent Sln trafficking is crucial for triggering apoptosis induced by extracellular butyrate. Given that LKB1 functions to control both epithelial polarity and cell death, we propose Sln is an important downstream target of LKB1.

Introduction

Monocarboxylates such as pyruvate, lactate, and butyrate were initially regarded as mere energy sources for cellular metabolism (Poole and Halestrap, 1993). However, recent studies suggested the crucial roles of monocarboxylates in diverse cellular processes including cell proliferation, differentiation, and apoptosis (for review see Halestrap and Meredith, 2004). The cellular transport of monocarboxlyates is facilitated by a family of transmembrane proteins, the monocarboxylate transporter (MCT) family (for review see Enerson and Drewes, 2003). Although significant advances have been made in understanding the biochemical properties of MCT (Galic et al., 2003; Lecona et al., 2008), little is known about the signaling pathways that regulate their physiological functions.

LKB1, a unique tumor suppressor that harbors protein kinase activity, was originally identified as a causative gene for Peutz-Jeghers syndrome, an autosomal dominant disease manifesting benign tumors in the gastrointestinal tract (Hemminki et al., 1998; Jenne et al., 1998). Previous studies established LKB1 as a master upstream kinase of the AMP-activated protein kinase (AMPK)/Par-1–related kinase family (Lizcano et al., 2004), which regulates multiple cellular physiologies such as energy homeostasis, cell division, and epithelial polarization (for review see Williams and Brenman, 2008). Moreover, recent genetic studies showed decreased apoptosis in Peutz-Jeghers syndrome patients and animal models (Karuman et al., 2001; Lee et al., 2006), implicating the vital function of LKB1 in regulating physiological cell death in vivo (Liang et al., 2007). However, the downstream executors mediating these physiological roles of LKB1 are poorly understood.

To find novel genes involved in the LKB1 signaling pathway, we performed a genetic modifier screen using *Drosophila melanogaster* (for review see St Johnston, 2002). Here, we identify an MCT, Silnoon (Sln), as a crucial downstream target of LKB1 in the control of cell death in polarized cells.

Results and discussion

To identify genetic interactors for LKB1, we prepared ~20,000 independent fly lines each possessing a randomly inserted EP element in their genome by mobilizing the transposable element with transposase expression (Fig. 1 A). We crossed these fly lines with LKB1-overexpressing flies and searched for the lines that modify the eye phenotype of LKB1 overexpression (Fig. 1 A).

Correspondence to Jongkyeong Chung: jchung@kaist.ac.kr

Abbreviations used in this paper: AMPK, AMP-activated protein kinase; AO, acridine orange; MCT, monocarboxylate transporter; rp49, ribosomal protein 49; Sln, Silnoon.

The online version of this article contains supplemental material.

The Rockefeller University Press $30.00
J. Cell Biol. Vol. 183 No. 1 11–17
www.jcb.org/cgi/doi/10.1083/jcb.200807052

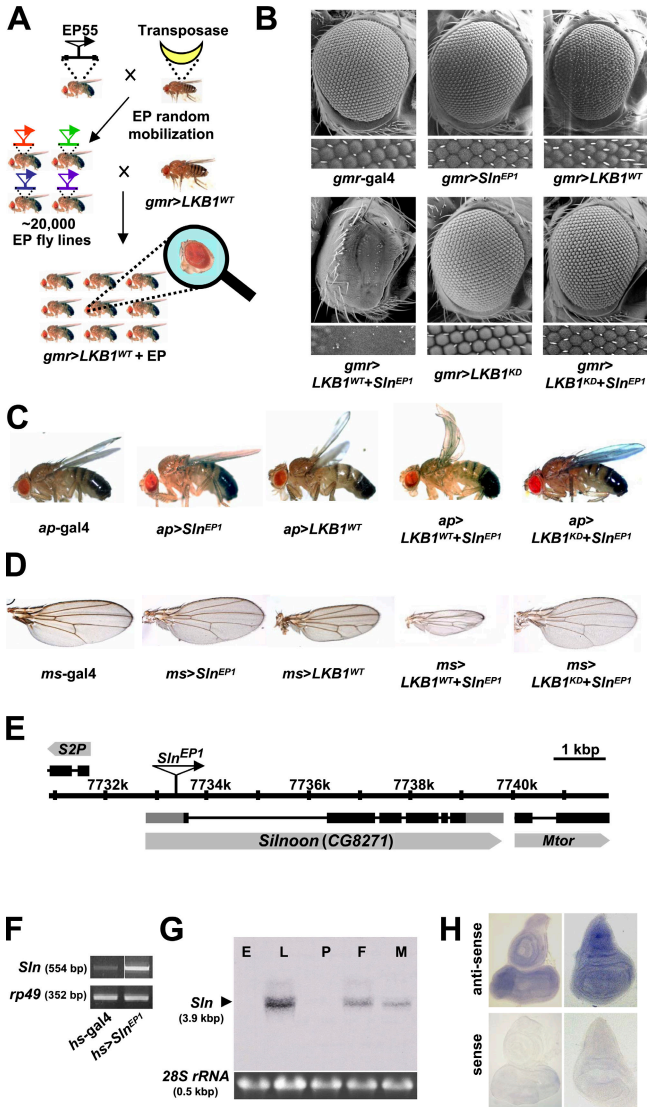

Figure 1. **A genetic modifier screen for *Drosophila* LKB1 identifies a novel LKB1-interacting gene, *Sln*.** (A) A schematic illustration of a genetic modifier screen for LKB1. (B–D) Scanning electron microscopy images of adult eyes (B) and images of adult wings (C and D) from the indicated genotypes. The penetrances of the eye and wing phenotypes were 100% (n = 100). (E) Genomic locus of the *Sln* gene. (F) RT-PCR analysis of *Sln* transcript in adult flies expressing *hs*-gal4 alone or *hs*-gal4–driven Sln^{EP1}. *rp49* was used as a loading control. (G) Developmental Northern blot analysis of *Sln*. E, embryo; L, larvae; P, pupa; F, adult female; M, adult male. *28S rRNA* was used as a loading control. (H) Whole-mount in situ hybridization analyses of *Sln* in wild-type larval eye (left) or wing (right) discs with an antisense (top) or a sense probe (bottom).

Among several candidate lines, we identified an EP line that dramatically enhanced the small and rough eye phenotypes of LKB1 overexpression (Fig. 1 B). We named a putative gene affected by this EP insertion as *Sln* (which means narrow eyes in Korean) and the EP insertion allele as Sln^{EP1}. Interestingly, *gmr*-gal4–driven Sln^{EP1} alone showed a normal eye phenotype (Fig. 1 B), indicating that the Sln^{EP1}-induced narrow eye phenotype completely depends on LKB1 coexpression. Remarkably, a kinase-dead form of LKB1 ($LKB1^{KD}$) did not exhibit any noticeable phenotype when expressed with Sln^{EP1} (Fig. 1 B), suggesting that the kinase activity of LKB1 is essential for its genetic interaction with Sln^{EP1}.

To investigate whether LKB1 also genetically interacts with Sln in other tissues, we expressed them in adult wings by using two distinct wing-specific gal4 drivers, dorsal-specific *apterous* (*ap*)-gal4 and wing pouch–specific *ms1096* (*ms*)-gal4. As a result, Sln^{EP1} strongly enhanced the upwardly curved and small wing phenotypes of the wild-type LKB1 ($LKB1^{WT}$), whereas it alone showed no obvious wing phenotypes (Fig. 1, C and D). In contrast, $LKB1^{KD}$ did not genetically interact with Sln^{EP1} (Fig. 1, C and D). These data suggest that the genetic relationship between LKB1 and Sln is conserved in various cell types.

We next performed inverse PCR analysis using genomic DNA carrying Sln^{EP1} to identify the gene affected by Sln^{EP1} and found that the EP element of Sln^{EP1} is inserted in the 5′-untranslated region of an uncharacterized gene, *CG8271* (Fig. 1 E). RT-PCR analysis indicated that Sln^{EP1} highly increased *CG8271* mRNA levels when induced by *heat shock* (*hs*)–gal4 driver (Fig. 1 F). However, the mRNA levels of other neighboring genes are not affected by Sln^{EP1} (unpublished data), implicating that *CG8271* is the gene specifically affected by Sln^{EP1}. Consistently, a transgenic allele of *CG8271* (Sln^{6}) showed the same genetic interaction with LKB1 as Sln^{EP1} (Fig. S1 A, available at http://www.jcb.org/cgi/content/full/jcb.200807052/DC1). Thus, we annotated the novel gene *CG8271* as *Sln*. Interestingly, Northern blot and whole-mount in situ hybridization analyses revealed that *Sln* transcript is highly expressed in larval and adult stages (Fig. 1 G) and broadly expressed in diverse tissues, including larval eye and wing imaginal discs (Fig. 1 H and Fig. S1 B).

To predict the molecular function of Sln, we searched for its sequence homologues from National Center for Biotechnology Information databases. Unexpectedly, a BLAST search conducted with the amino acid sequence of Sln identified several MCT proteins. Alignments of Sln with human and mouse MCTs (Fig. S1 C) showed that 12 transmembrane domains, two sugar transporter domains, and a large intracellular loop between the sixth and seventh transmembrane domains, which are the key features of the MCT family (for review see Enerson and Drewes, 2003), are all well conserved in Sln (Fig. 2, A and B).

To examine whether Sln functions as an MCT protein in *Drosophila*, we chose two naturally occurring substrates of MCT, butyrate and lactate, which are known to exist in the insect body (Kane and Breznak, 1991; Santo Domingo et al., 1998; Lemke et al., 2003). We measured the amounts of [^{14}C]butyrate and [^{14}C]lactate uptake by larval wing discs expressing wild-type Sln (Sln^{6}) or a mutant form of Sln (Sln^{G366V}) that possesses a point mutation causing reduced transport activity (Fig. 2 B; Galic et al., 2003). Notably, Sln^{6}-expressing wing discs transported much higher amounts of butyrate and lactate than the control wing discs (Fig. 2 C). However, Sln^{G366V}-expressing discs showed lower monocarboxylate uptake compared with Sln^{6}, despite similar expression levels of these proteins (Fig. 2 C and not depicted). Interestingly, coexpression of LKB1 enhanced Sln-mediated monocarboxylate transport (Fig. 2 D), which is consistent with the genetic interaction between LKB1 and Sln (Fig. 1, B–D). These results suggest that Sln possesses butyrate and lactate transport activities in *Drosophila* tissues.

Because LKB1 and Sln synergistically reduced the eye size of adult flies (Fig. 1 B), we examined the larval eye discs to

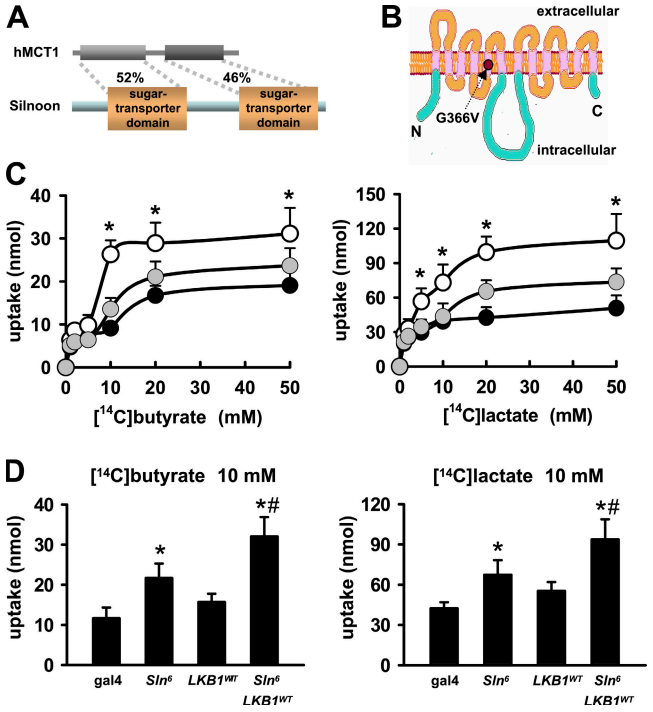

Figure 2. **Sln transports butyrate and lactate in *Drosophila* tissues.** (A) Amino acid sequence similarities (%) of Sln with human MCT1 (hMCT1). (B) A schematic topology of Sln. An arrow indicates the location of a highly conserved glycine residue mutated to valine in the Sln^{G366V} allele. (C) Quantification of the amounts of [^{14}C]butyrate (left) and [^{14}C]lactate (right) uptake by larval wing discs expressing *ms*-gal4 alone (black), *ms*-gal4–driven Sln^{6} (white), or Sln^{G366V} (gray) at varying concentrations (1–50 mM) of each monocarboxylate. Error bars show the SD of five independent samples. *, P < 0.05 versus *ms*-gal4 alone. (D) Quantification of the amounts of [^{14}C]butyrate (left) and [^{14}C]lactate (right) uptake by wing discs expressing *ms*-gal4 alone, *ms*-gal4–driven Sln^{6}, $LKB1^{WT}$, or both Sln^{6} and $LKB1^{WT}$ (from left to right) at 10 mM of each monocarboxylate. Error bars show the SD of five independent samples. *, P < 0.05 versus *ms*-gal4 alone; #, P < 0.05 versus *ms*>Sln^{6}.

understand the cellular process responsible for these phenotypes. BrdU incorporation analysis and phosphohistone H3 immunostaining revealed that neither LKB1 nor Sln expression affects G1/S and G2/M cell cycle progression, respectively (Fig. 3 A, top and middle). Furthermore, a neuronal-specific Elav immunostaining showed no differentiation defect in LKB1- and Sln-expressing eye discs (Fig. 3 A, bottom). We also generated flipped-out mosaic clones expressing LKB1 and Sln simultaneously (Fig. 3 B). These mitotic clones marked by cytoplasmic GFP showed similar cell size to that of neighboring GFP-negative cells in larval fat body (Fig. 3 B, top). However, the area of mitotic clones was gradually decreased 48 h after clonal induction, implicating that these clones were selectively eliminated by unknown cell death mechanisms (Fig. 3 B, bottom). To examine this, we performed TUNEL and acridine orange (AO) staining to detect cells undergoing apoptosis (Fig. 3 C). Remarkably, Sln^{EP1} strongly enhanced the apoptosis in LKB1-expressing eye discs, whereas it alone showed no significant apoptotic signals (Fig. 3 C). Furthermore, coexpression of either apoptosis blocker, *Drosophila* inhibitor of apoptosis or p35, considerably suppressed the apoptotic cell death induced by LKB1 and Sln coexpression (Fig. 3 D). These results indicate that Sln specifically

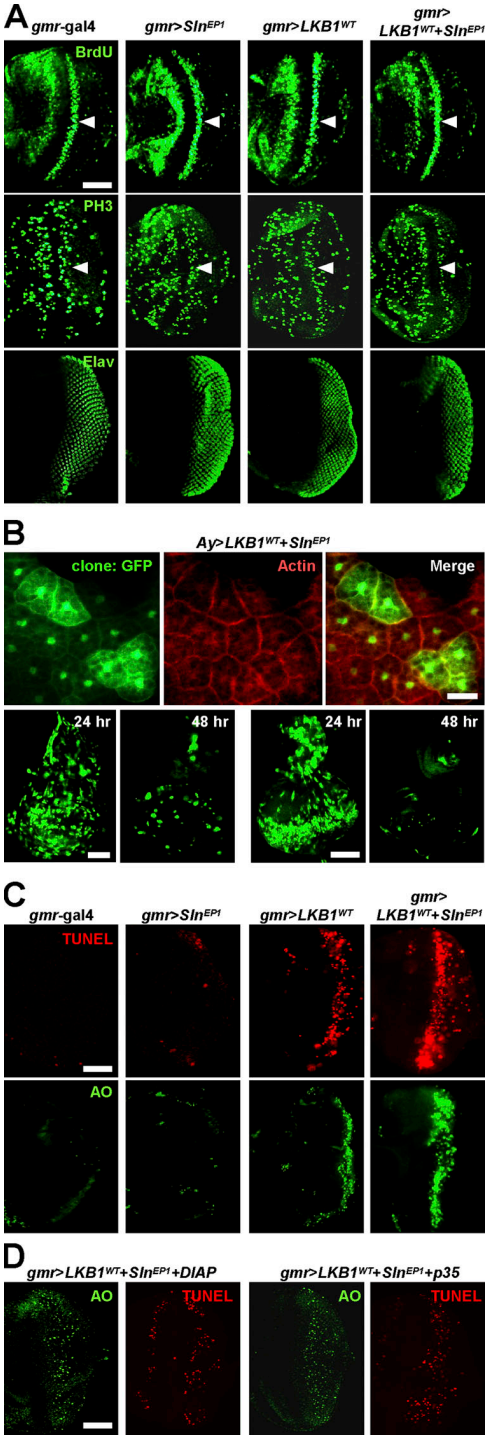

Figure 3. **Sln enhances LKB1-dependent apoptosis without affecting cell cycle progression or cell size.** (A) Immunostaining against BrdU (top), phosphohistone H3 (middle), or Elav (bottom) in larval eye discs from the indicated genotypes. Arrowheads mark the second mitotic wave posterior to the morphogenetic furrow. Posterior at right. (B) Cytoplasmic GFP-marked flipped-out mitotic clones expressing LKB1 and Sln in larval fat body (top), wing disc (bottom left), or eye disc (bottom right). Filamentous actin was stained in fat body (top, red). Nuclear GFP is nonspecific autofluorescence in fat body (top). The time after clonal induction is indicated (bottom). (C and D) TUNEL (red) and AO (green) staining in larval eye discs from the indicated genotypes. The penetrances of apoptosis phenotypes were 100% (n = 10). Posterior at right. Bars, 50 µm.

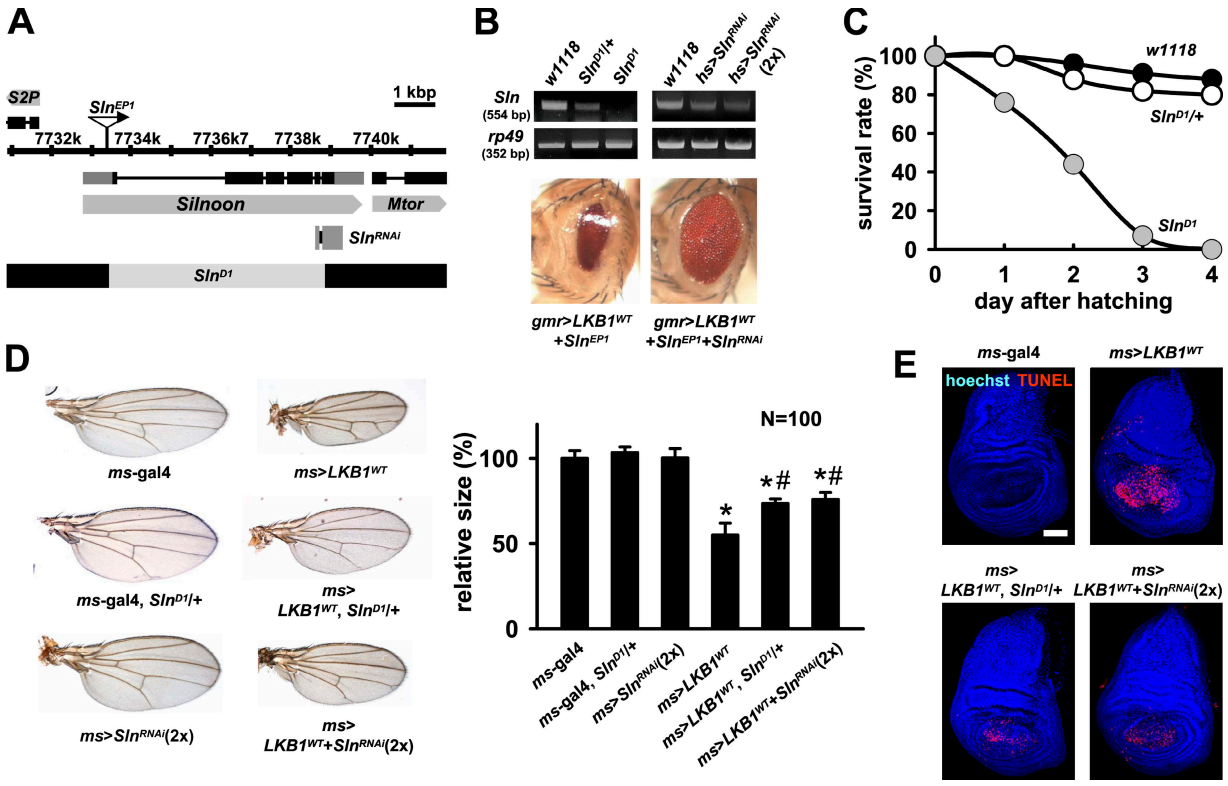

Figure 4. **Sln loss-of-function mutants suppress LKB1-dependent apoptosis.** (A) Genomic locus of *Sln* gene. The deletion and targeting regions of the Sln^{D1} and the Sln^{RNAi} allele are indicated. (B) RT-PCR analyses of *Sln* transcript in wild-type (*w1118*), Sln^{D1} heterozygous, or Sln^{D1} homozygous mutant larvae (top left) and in adult flies expressing one copy or two copies of *hs*-gal4–driven Sln^{RNAi} (top right). *rp49* was used as a loading control. Microscopy images of adult eyes expressing *gmr*-gal4–driven $LKB1^{WT}$ and Sln^{EP1} without (bottom left) or with (bottom right) Sln^{RNAi}. (C) Survival rates of wild-type (black), Sln^{D1} heterozygous (white), and Sln^{D1} homozygous (gray) mutant larvae. (D) Microscopy images of adult wing preparations from the indicated genotypes (left) and the quantification of relative wing sizes (right). Error bars show the SD of 100 independent samples. *, $P < 0.05$ versus *ms*-gal4 alone; #, $P < 0.05$ versus *ms*>$LKB1^{WT}$. (E) TUNEL (red) and hoechst (DNA; blue) staining in larval wing discs from the indicated genotypes. Bar, 50 μm.

augments LKB1-dependent apoptosis without affecting cell growth and proliferation.

To further investigate the endogenous role of *Sln*, we generated various loss-of-function mutants of *Sln*. We made a genomic deletion mutant of *Sln* (Sln^{D1}), whose exons 1–5 are removed by imprecise excision of Sln^{EP1} (Fig. 4 A). In addition, we constructed an inducible RNA interference allele of *Sln* (Sln^{RNAi}) that generates double-stranded RNA targeted to the 3′ region of *Sln* mRNA when induced by gal4 drivers (Fig. 4 A). RT-PCR analyses showed that *Sln* mRNA expression was completely absent in homozygous Sln^{D1} larvae and markedly decreased in adult flies expressing Sln^{RNAi} in a copy number–dependent manner (Fig. 4 B, top). Efficacy of Sln^{RNAi} allele was also confirmed by its dramatic suppressive effect on the narrow eye phenotype induced by LKB1 and Sln coexpression (Fig. 4 B, bottom).

Sln^{D1} homozygous mutant larvae died within 4 d after hatching from embryos (Fig. 4 C), suggesting that Sln is important for early larval development. The mutant larvae halted food uptake a few hours after hatching and showed accumulation of blue dye–mixed food mostly in the hindgut region (Fig. S2 A, available at http://www.jcb.org/cgi/content/full/jcb.200807052/DC1). Moreover, they displayed smaller body size and severely reduced peristaltic movement compared with the control larvae (Fig. S2, A and B). These phenotypes were similarly observed in Sln^{D1} heterozygote combined with the deficiencies covering the *Sln* genomic region (*Df(2R)BSC329* and *Df(2R)ED2247*; unpublished data), supporting that Sln^{D1} is a loss-of-function allele of *Sln*. Together with the highest expression of *Sln* at the larval stage (Fig. 1 G), these results suggest that Sln is important for transporting metabolic monocarboxylates as energy sources for larval growth and development.

Because Sln^{D1} homozygous mutant showed early lethality, we used Sln^{D1} heterozygous mutant and the Sln^{RNAi} allele to investigate the signaling hierarchy between LKB1 and Sln. By epistatic analyses in adult wings, we found that LKB1-dependent reduced wing size was markedly restored in Sln^{D1} heterozygous genetic background (Fig. 4 D). Consistently, down-regulation of *Sln* using two copies of Sln^{RNAi} also restored the reduced wing size by LKB1 expression (Fig. 4 D). This Sln^{D1}- or Sln^{RNAi}-mediated phenotypic rescue was caused by the decreased apoptosis in LKB1-expressing larval discs without changes in LKB1 protein levels (Fig. 4 E and Fig. S2, C and D). These data suggest that Sln acts downstream of LKB1 to mediate the pro-apoptotic role of LKB1 in the control of tissue size.

The activity of MCT can be regulated by its expression level, membrane trafficking, and posttranslational modification (for review see Enerson and Drewes, 2003). To investigate the

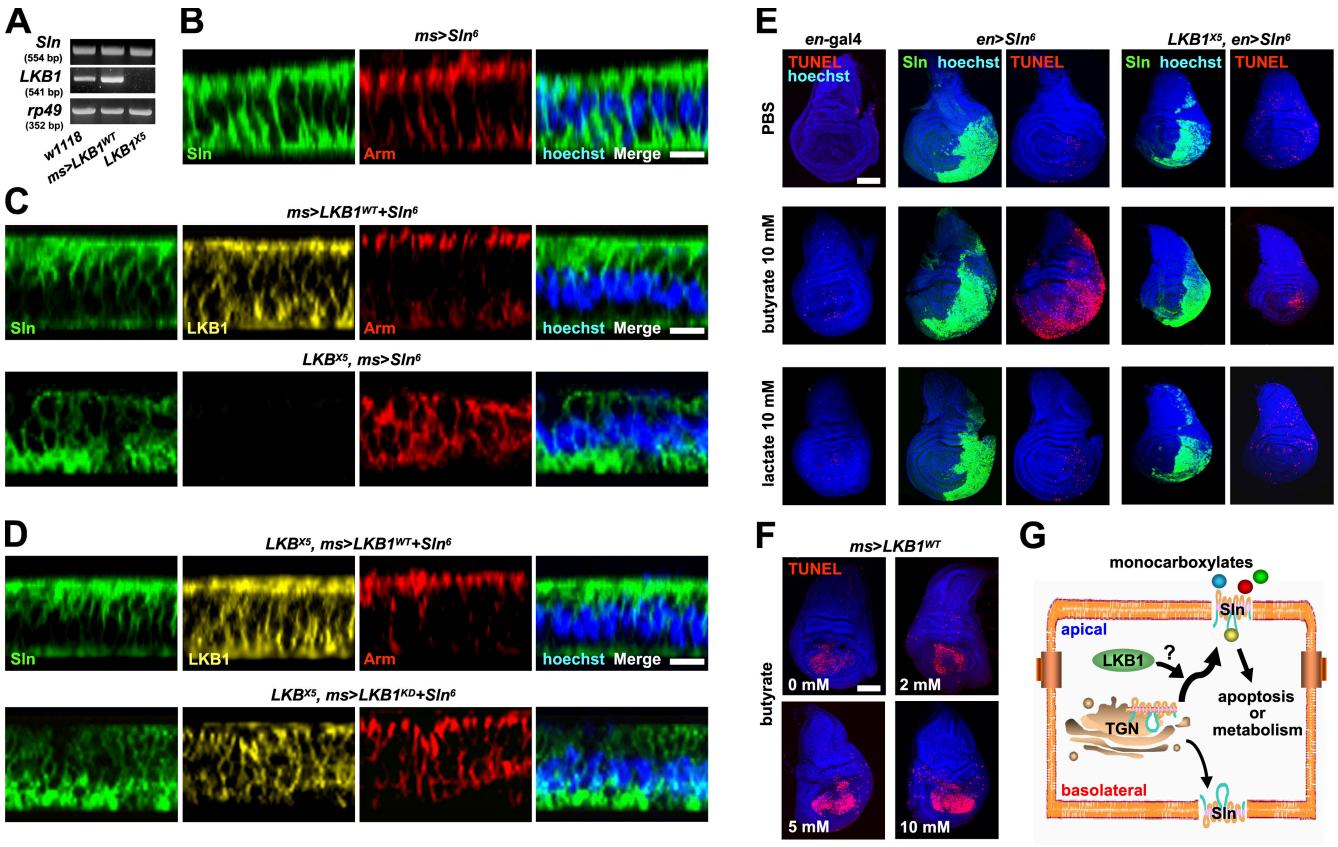

Figure 5. **LKB1 induces apical trafficking of Sln to mediate butyrate-induced apoptosis.** (A) RT-PCR analyses of *Sln* and *LKB1* transcripts in larval wing discs from the indicated genotypes. *rp49* was used as a loading control. (B–D) Confocal z-stack analyses of the immunostaining against Myc (Sln; green), LKB1 (yellow), armadillo (Arm; red), and hoechst (DNA; blue) in larval wing discs from the indicated genotypes. The penetrances of Sln polarity phenotypes were 100, 100, 73, 100, and 67% (from top to bottom), respectively (n = 15). Bars, 5 µm. (E and F) TUNEL (red) and hoechst (DNA; blue) staining and Myc (Sln; green) immunostaining in larval wing discs from the indicated genotypes after stimulation with the indicated concentrations of butyrate or lactate. Bars, 50 µm. (G) A proposed model of the interplay between LKB1 and Sln in polarized cells. LKB1 induces apical trafficking of Sln, promoting the transport of extracellular monocarboxylates that may act as metabolites or apoptosis inducers. TGN, trans-Golgi networks.

mechanism of interplay between LKB1 and Sln, we examined whether LKB1 regulates the expression level of Sln. However, neither endogenous mRNA nor exogenous protein level of Sln was altered in LKB1-overexressing or -deficient (LKB^{X5}; Lee et al., 2006) larval wing discs (Fig. 5 A and not depicted). We also investigated whether LKB1 regulates the subcellular localization of Sln. Because we failed to generate antibodies detecting endogenous Sln, we alternatively examined the localization of transgenic Sln in larval wing discs. Confocal z-stack analysis of immunostaining against Sln and apical marker armadillo showed that Sln is localized both in the apical and basolateral membranes of polarized epithelial cells (Fig. 5 B). Strikingly, LKB1 expression induced the asymmetrical localization of Sln predominantly in the apical side of the wing epithelium (Fig. 5 C, top). In contrast, absence of LKB1 caused the localization of Sln largely in the basolateral side of the wing epithelium (Fig. 5 C, bottom). These results suggest that LKB1 induces apical trafficking of Sln in epithelial cells. We also compared the effect of $LKB1^{WT}$ and $LKB1^{KD}$ on Sln localization in the LKB1-null genetic background. Consistent with these results (Fig. 5 C, top), $LKB1^{WT}$ induced apical localization of Sln in LKB1-deficient epithelial cells (Fig. 5 D, top). However, $LKB1^{KD}$ failed to provoke this specific effect (Fig. 5 D, bottom), indicating that the kinase activity is essential for LKB1 to induce apical trafficking of Sln.

Targeted delivery of MCT in polarized cells is crucial for their transport of extracellular monocarboxylates that may exert various physiological processes in the cells (for review see Morris and Felmlee, 2008). Because LKB1 induces apical trafficking of Sln (Fig. 5, C and D) and Sln mediates LKB1-dependent apoptosis (Fig. 4 D), we examined whether LKB1 promotes apical trafficking of Sln to induce apoptosis. Using TUNEL staining in ex vivo–cultured wing discs, we examined the degree of apoptosis upon treatment with each Sln substrate, butyrate and lactate. Surprisingly, incubation of wing discs with butyrate caused massive apoptosis in the Sln-expressing regions by posterior-specific *engrailed* (*en*)-gal4 (Fig. 5 E, middle). However, lactate induced no significant death signals in Sln-expressing wing discs compared with control (Fig. 5 E, left and middle). Remarkably, this Sln-mediated apoptosis upon butyrate treatment was considerably suppressed in LKB1-null genetic background (Fig. 5 E, right). In addition, LKB1-induced apoptosis was further enhanced by butyrate treatment (Fig. 5 F and Fig. S3, available at http://www.jcb.org/cgi/content/full/jcb.200807052/DC1). These data suggest that LKB1-dependent

apical trafficking of Sln is critical in mediating the butyrate-induced apoptosis.

In this study, we show that Sln, a *Drosophila* MCT protein transporting butyrate and lactate, is a key executor of apoptosis as a downstream mediator of tumor suppressor LKB1. The kinase activity of LKB1 induces apical trafficking of Sln in polarized cells, and this may promote Sln to transport extracellular butyrate, which can provoke apoptosis.

Our ex vivo tissue culture data showed that endogenous Sln can enhance LKB1-induced apoptosis by >5 mM of butyrate treatment (Fig. 5 F). This amount is consistent with the concentration of monocarboxylates (0.5–6 mM) in the insect hemolymph produced by resident bacterial flora in the gut (Kane and Breznak, 1991; Santo Domingo et al., 1998; Lemke et al., 2003). These monocarboxylates, including butyrate, might be delivered to various Sln-expressing organs through the *Drosophila* open circulatory system. It is well established that butyrate acts as an endogenous stimulator of epithelial cell death via diverse cellular mechanisms, such as inhibition of histone deacetylase and activation of p53- or Fas-dependent apoptosis (for review see Gupta et al., 2006). In fact, impaired butyrate uptake causes poor differentiation and defective cellular turnover, leading to various human cancers (for review see Gupta et al., 2006; Paroder et al., 2006).

Consistent with the previous results (Shaw et al., 2004; Lee et al., 2006), our data also indicate that the kinase activity of LKB1 is crucial in its biological effects: the induction of apoptosis (Fig. 3 C) and the regulation of Sln localization (Fig. 5 D). These results implicate that phosphorylation events are involved in the control of Sln by LKB1. In this scenario, the phosphorylation target could be Sln itself or other unknown binding partners of Sln. It is also possible that LKB1 directly phosphorylates the target protein or does so via its downstream kinases such as Par-1 and AMPK. Indeed, Par-1 was known to promote apical protein trafficking in polarized kidney cell lines (Cohen et al., 2004). Alternatively, AMPK could be another potential mediator of Sln trafficking because it regulates not only epithelial polarity but also energy homeostasis (Lee et al., 2007) that possibly controls the transport of metabolic monocarboxylates. Further studies are necessary to disclose the mechanism of Sln localization regulated by the LKB1-dependent signaling cascade.

The proper control of programmed cell death is critical in maintaining tissue homeostasis and preventing tumor formation (for review see Radtke and Clevers, 2005). Importantly, MCT also participates in these physiological processes by stimulating epithelial turnover via butyrate-dependent apoptosis (Cuff et al., 2005; Natoni et al., 2005). Because trafficking and anchoring of MCT proteins to a specific cellular compartment are essential for their proper function (Kirk et al., 2000; Deora et al., 2005), the LKB1-dependent apical trafficking of Sln and subsequent induction of apoptosis might illustrate a potential control mechanism for MCT-mediated epithelial turnover in human tissues (Fig. 5 G). Interestingly, LKB1 also stimulates physiological apoptosis as a master tumor suppressor in intestinal epithelium (for review see Yoo et al., 2002). In these regards, our present study proposes a plausible link between the two previously unrelated players of apoptosis, LKB1 and MCT, and suggests a possible mechanism to relate epithelial polarization to cell death control by LKB1.

Materials and methods

Drosophila strains

Sln^{D1} was generated by imprecise excision of Sln^{EP1} allele. Deletion site of Sln^{D1} (~6-kbp deletion, including translation initiation site and exons 1–5) was determined by genomic PCR analysis. Myc-tagged Sln^{6} and Sln^{G366V} were subcloned into the pUAST vector and microinjected into *w1118* embryos. To generate Sln^{RNAi}, cDNA against 2,072–2,565 bp of the *Sln*-coding sequence was subcloned into the SympUAST vector and microinjected into *w1118* embryos. $LKB1^{X5}$, $UAS\text{-}LKB1^{WT}$, $UAS\text{-}LKB1^{KD}$, and *UAS-DIAP* lines were described previously (Lee et al., 2006). The gal4 lines, *UAS-p35* line, EP element (*EP55*), *Δ2-3*, *Act>CD2>gal4 UAS-GFP,* deficiency lines, and *heat-shock flippase* (*hs-FLP*) were obtained from the Bloomington Stock Center.

Antibodies

C-terminal protein (amino acids 468–567) of *Drosophila* LKB1 was used to generate anti-LKB1 guinea pig antisera. Anti-armadillo, anti-tubulin, anti-BrdU, anti-Elav, and anti-Myc antibodies were purchased from the Developmental Studies Hybridoma Bank. Anti–phosphohistone H3 antibody was purchased from Millipore. TRITC-labeled phalloidin (Sigma-Aldrich) and Hoechst 33258 (Sigma-Aldrich) were used to visualize filamentous actins and DNA, respectively.

RT-PCR analyses

RNA was extracted using Easy-Blue (Intron Biotechnology) and reverse transcribed using *Maxime* RT premix kit (Intron Biotechnology). The following primers were used to amplify *Sln*, *LKB1*, or *ribosomal protein 49* (*rp49*) transcripts by PCR, respectively: 5′-GTGAGGCGGGATACCTGGTGG-3′ and 5′-GGCCTCCTCGCACTCCTC-3′; 5′-CTAGCTCTCGGCCAGTCG-GAGG-3′ and 5′-GCCGTACGATCCCTCGCCGAG-3′; and 5′-TCTCGCC-GCAGTAAAC-3′ and 5′-TGACCATCCGCCCAGCATACA-3′.

Mutagenesis

Site-directed mutagenesis was performed using the Quick change site-directed mutagenesis kit (Stratagene) with the following primer: 5′-GGAATCT-GCGTTTCGG**T**CACTGCCGCCGGCAGC-3′ (G→T, Gly366Val). Only the sense primer is shown. Bold indicates the mutated nucleotide.

Histology and molecular analyses

Protein extraction and immunoblot analysis were performed as previously described (Kim et al., 2000). Immunostaining and whole-mount in situ hybridization analyses were performed as previously described (Kim et al., 2004). Northern blot analysis was performed as previously described (Lee et al., 2001). A 494-bp fragment (nucleotides 2072–2565) of *Sln*-coding sequence was used as a hybridization probe. TUNEL staining was performed using the in situ cell death detection kit (Roche). For AO staining, third instar larvae were dissected in PBS and incubated in 1.6×10^{-6} M AO solution (EMD) for 5 min at 25°C. The samples were washed with PBS and mounted on the coverslip. For heat-shock induction, adult flies were incubated at 37°C for 2 h and allowed to recover at 25°C for 1 h. Flipped-out mitotic clones were generated by crossing *Act>CD2>gal4 UAS-GFP* virgins with males carrying *hs-FLP*, $UAS\text{-}LKB1^{WT}$, and Sln^{EP1}. FLP-mediated excision of the CD2 insert was induced by heat shock at 37°C for 1 h.

Monocarboxylate transport experiments

Third instar larval wing discs were isolated in PBS and incubated in M3 insect medium (Sigma-Aldrich) at pH 7.5 for 30 min at 25°C. The tissues were then incubated with M3 medium at pH 6.5 containing varying concentrations of [^{14}C]butyrate (60 mCi/mmol; ARC Inc.) or [^{14}C]lactate (161 mCi/mmol; GE Healthcare) for 5 min at 25°C (Lecona et al., 2008). The uptake was stopped by three washes with ice-cold PBS. The tissues were permeabilized with 0.3% Triton X-100 in PBS for 10 min and the amounts of radioactive monocarboxylates in the solution were measured by liquid scintillation counting in a β counter (PerkinElmer). The remaining tissues were subjected to immunoblot analysis to measure Sln protein levels. For TUNEL staining, wing discs were incubated with M3 medium at pH 7.5 for 30 min at 25°C and transferred to M3 medium at pH 6.5 containing varying concentrations of butyrate or lactate (Sigma-Aldrich) for 6 h at 25°C. The tissues were then subjected to TUNEL and immunostaining as previously described (Lee et al., 2006). P-values were calculated by one-way analysis of variance.

Microscopy

Confocal images were acquired at 21°C using a microscope (LSM 510 META) and LSM image browser v.3.2 SP2 software (Carl Zeiss, Inc.). Plan-Neofluar 20x (0.5 NA) and C-Apochromat 40x (1.20 NA, water medium) objective lenses were used (Carl Zeiss, Inc.). FITC, GFP, TRITC, Cy5, and Hoechst 33258 fluorochromes were used. Other microscopy images were acquired using a digital camera (AxioCam) and AxioVS40AC v.4.4 software (Carl Zeiss, Inc.). Scanning electron microscopy images were obtained by LEO1455VP (Carl Zeiss, Inc.) in a variable pressure secondary electron mode. Images were processed in Photoshop v.7.0 (Adobe).

Online supplemental material

Fig. S1 shows the genetic interaction between LKB1 and transgenic Sln, the expression pattern of Sln, and sequence alignment of Sln with mammalian MCTs. Fig. S2 shows the behavior phenotypes of Sln^{D1} larvae and the effect of Sln down-regulation on LKB1-induced apoptosis. Fig. S3 shows quantification of LKB1-induced apoptosis enhanced by varying concentrations of butyrate treatment. Online supplemental material is available at http://www.jcb.org/cgi/content/full/jcb.200807052/DC1.

This work was supported by a National Creative Research Initiatives grant (R16-2001-002-01000-0) from Korea Science and Engineering Foundation/ Ministry of Education, Science, and Technology.

The authors have no conflicting financial interests.

Submitted: 9 July 2008
Accepted: 10 September 2008

References

Cohen, D., E. Rodriguez-Boulan, and A. Müsch. 2004. Par-1 promotes a hepatic mode of apical protein trafficking in MDCK cells. *Proc. Natl. Acad. Sci. USA.* 101:13792–13797.

Cuff, M., J. Dyer, M. Jones, and S.P. Shirazi-Beechey. 2005. The human colonic monocarboxylate transporter isoform 1: its potential importance to colonic tissue homeostasis. *Gastroenterology.* 128:676–686.

Deora, A.A., N. Philp, J. Hu, D. Bok, and E. Rodriguez-Boulan. 2005. Mechanisms regulating tissue-specific polarity of monocarboxylate transporters and their chaperone CD147 in kidney and retinal epithelia. *Proc. Natl. Acad. Sci. USA.* 102:16245–16250.

Enerson, B.E., and L.R. Drewes. 2003. Molecular features, regulation, and function of monocarboxylate transporters: implications for drug delivery. *J. Pharm. Sci.* 92:1531–1544.

Galic, S., H.P. Schneider, A. Broer, J.W. Deitmer, and S. Broer. 2003. The loop between helix 4 and helix 5 in the monocarboxylate transporter MCT1 is important for substrate selection and protein stability. *Biochem. J.* 376:413–422.

Gupta, N., P.M. Martin, P.D. Prasad, and V. Ganapathy. 2006. SLC5A8 (SMCT1)-mediated transport of butyrate forms the basis for the tumor suppressive function of the transporter. *Life Sci.* 78:2419–2425.

Halestrap, A.P., and D. Meredith. 2004. The SLC16 gene family—from monocarboxylate transporters (MCTs) to aromatic amino acid transporters and beyond. *Pflugers Arch.* 447:619–628.

Hemminki, A., D. Markie, I. Tomlinson, E. Avizienyte, S. Roth, A. Loukola, G. Bignell, W. Warren, M. Aminoff, P. Höglund, et al. 1998. A serine/threonine kinase gene defective in Peutz-Jeghers syndrome. *Nature.* 391:184–187.

Jenne, D.E., H. Reimann, J. Nezu, W. Friedel, S. Loff, R. Jeschke, O. Müller, W. Back, and M. Zimmer. 1998. Peutz-Jeghers syndrome is caused by mutations in a novel serine threonine kinase. *Nat. Genet.* 18:38–43.

Kane, M.D., and J.A. Breznak. 1991. Effect of host diet on production of organic acids and methane by cockroach gut bacteria. *Appl. Environ. Microbiol.* 57:2628–2634.

Karuman, P., O. Gozani, R.D. Odze, X.C. Zhou, H. Zhu, R. Shaw, T.P. Brien, C.D. Bozzuto, D. Ooi, L.C. Cantley, and J. Yuan. 2001. The Peutz-Jegher gene product LKB1 is a mediator of p53-dependent cell death. *Mol. Cell.* 7:1307–1319.

Kim, M., G.H. Cha, S. Kim, J.H. Lee, J. Park, H. Koh, K.Y. Choi, and J. Chung. 2004. MKP-3 has essential roles as a negative regulator of the Ras/mitogen-activated protein kinase pathway during *Drosophila* development. *Mol. Cell. Biol.* 24:573–583.

Kim, S., Y. Jung, D. Kim, H. Koh, and J. Chung. 2000. Extracellular zinc activates p70 S6 kinase through the phosphatidylinositol 3-kinase signaling pathway. *J. Biol. Chem.* 275:25979–25984.

Kirk, P., M.C. Wilson, C. Heddle, M.H. Brown, A.N. Barclay, and A.P. Halestrap. 2000. CD147 is tightly associated with lactate transporters MCT1 and MCT4 and facilitates their cell surface expression. *EMBO J.* 19:3896–3904.

Lecona, E., N. Olmo, J. Turnay, A. Santiago-Gómez, I. López de Silanes, M. Gorospe, and M.A. Lizarbe. 2008. Kinetic analysis of butyrate transport in human colon adenocarcinoma cells reveals two different carrier-mediated mechanisms. *Biochem. J.* 409:311–320.

Lemke, T., U. Stingl, M. Egert, M.W. Friedrich, and A. Brune. 2003. Physicochemical conditions and microbial activities in the highly alkaline gut of the humus-feeding larva of *Pachnoda ephippiata* (Coleoptera: Scarabaeidae). *Appl. Environ. Microbiol.* 69:6650–6658.

Lee, J.H., K.S. Cho, J. Lee, J. Yoo, J. Lee, and J. Chung. 2001. Diptericin-like protein: an immune response gene regulated by the anti-bacterial gene induction pathway in *Drosophila. Gene.* 271:233–238.

Lee, J.H., H. Koh, M. Kim, J. Park, S.Y. Lee, S. Lee, and J. Chung. 2006. JNK pathway mediates apoptotic cell death induced by tumor suppressor LKB1 in *Drosophila. Cell Death Differ.* 13:1110–1122.

Lee, J.H., H. Koh, M. Kim, Y. Kim, S.Y. Lee, R.E. Karess, S.H. Lee, M. Shong, J.M. Kim, J. Kim, and J. Chung. 2007. Energy-dependent regulation of cell structure by AMP-activated protein kinase. *Nature.* 447:1017–1020.

Liang, J., S.H. Shao, Z.X. Xu, B. Hennessy, Z. Ding, M. Larrea, S. Kondo, D.J. Dumont, J.U. Gutterman, C.L. Walker, et al. 2007. The energy sensing LKB1-AMPK pathway regulates p27(kip1) phosphorylation mediating the decision to enter autophagy or apoptosis. *Nat. Cell Biol.* 9:218–224.

Lizcano, J.M., O. Goransson, R. Toth, M. Deak, N.A. Morrice, J. Boudeau, S.A. Hawley, L. Udd, T.P. Makela, D.G. Hardie, and D.R. Alessi. 2004. LKB1 is a master kinase that activates 13 kinases of the AMPK subfamily, including MARK/PAR-1. *EMBO J.* 23:833–843.

Morris, M.E., and M.A. Felmlee. 2008. Overview of the proton-coupled MCT (SLC16A) family of transporters: characterization, function and role in the transport of the drug of abuse gamma-hydroxybutyric acid. *AAPS J.* 10:311–321.

Natoni, F., L. Diolordi, C. Santoni, and M.S. Gilardini Montani. 2005. Sodium butyrate sensitizes human pancreatic cancer cells to both the intrinsic and the extrinsic apoptotic pathways. *Biochim. Biophys. Acta.* 1745:318–329.

Paroder, V., S.R. Spencer, M. Paroder, D. Arango, S. Schwartz, J.M. Mariadason, L.H. Augenlicht, S. Eskandari, and N. Carrasco. 2006. Na(+)/monocarboxylate transport (SMCT) protein expression correlates with survival in colon cancer: molecular characterization of SMCT. *Proc. Natl. Acad. Sci. USA.* 103:7270–7275.

Poole, R.C., and A.P. Halestrap. 1993. Transport of lactate and other monocarboxylates across mammalian plasma membranes. *Am. J. Physiol.* 264:C761–C782.

Radtke, F., and H. Clevers. 2005. Self-renewal and cancer of the gut: two sides of a coin. *Science.* 307:1904–1909.

Santo Domingo, J.W., M.G. Kaufman, M.J. Klug, W.E. Holben, D. Harris, and J.M. Tiedje. 1998. Influence of diet on the structure and function of the bacterial hindgut community of crickets. *Mol. Ecol.* 7:761–767.

Shaw, R.J., M. Kosmatka, N. Bardeesy, R.L. Hurley, L.A. Witters, R.A. DePinho, and L.C. Cantley. 2004. The tumor suppressor LKB1 kinase directly activates AMP-activated kinase and regulates apoptosis in response to energy stress. *Proc. Natl. Acad. Sci. USA.* 101:3329–3335.

St Johnston, D. 2002. The art and design of genetic screens: *Drosophila melanogaster. Nat. Rev. Genet.* 3:176–188.

Williams, T., and J.E. Brenman. 2008. LKB1 and AMPK in cell polarity and division. *Trends Cell Biol.* 18:193–198.

Yoo, L.I., D.C. Chung, and J. Yuan. 2002. LKB1—a master tumour suppressor of the small intestine and beyond. *Nat. Rev. Cancer.* 2:529–535.